

## Electrochemical Behavior of Alloy 600 and Magnetite in Solutions of Sulfate and Thiosulfate

Je Oh Han<sup>a,b</sup>, Geun Dong Song<sup>a</sup>, Soon-Hyeok Jeon<sup>a</sup>, Jong Hyeon Lee<sup>b</sup>, Do Haeng Hur<sup>a,\*</sup>  
<sup>a</sup> Nuclear Materials Research Division, Korea Atomic Energy Research Institute, 989-111 Daedeok-daero,  
Yuseong-gu, Daejeon 34057, Republic of Korea  
<sup>b</sup> Department of Advanced Materials Engineering, Chungnam National University, 99 Daehak-ro,  
Yuseong-gu, Daejeon, 34134, Republic of Korea  
\*Corresponding author: dhhur@kaeri.re.kr

### 1. Introduction

Because the secondary coolant system in pressurized water reactors (PWRs) is mostly composed of carbon steel, magnetite is the major corrosion products in the secondary coolant system [1]. Magnetite is released from carbon steel surface, transported by feed water, and deposited on the steam generator tube surfaces and tube support plates. The morphology of the magnetite deposits has many pores. Therefore, some impurities are concentrated in the pores [2]. Aggressive chemical impurities such as sulfur oxyanions and chloride ions are concentrated into the porous magnetite deposits by local boiling. These phenomena accelerate the corrosion of the steam generator tube [3]. Among many of the impurities, sulfur can be originated from feed water and resin source. [4]. Sulfur can exist in many valence states, such as  $-2$  ( $S^{2-}$ ),  $+2$  ( $S_2O_3^{2-}$ ),  $+4$  ( $SO_3^{2-}$ ) and  $+6$  ( $SO_4^{2-}$ ). Reduced forms of sulfur can cause IGA and pitting of high-nickel alloys like Alloy 600. Sulfate ions can also accelerate local attack of Alloy 600 during cold shutdown conditions [5-6].

Recently, we have reported that general corrosion of carbon steel and Ni-based alloys is significantly accelerated by a galvanic effect between the materials and magnetite in various environments [7-11]. Song et al. have also reported that the corrosion of Alloy 690 is accelerated by synergistic effect of magnetite and chloride ions [12]. However, the effect of sulfur oxyanions has not been considered in evaluating the effect of magnetite on the corrosion behavior of Alloy 600 until now. The objective of this research is to assess the synergistic effect of sulfur oxyanions (sulfate and thiosulfate) and magnetite on the corrosion of Alloy 600. In order to investigate electrochemical behavior of magnetite itself, magnetite specimens were prepared by an electrodeposition method. The electrochemical corrosion behavior of Alloy 600 and magnetite were evaluated by using potentiodynamic polarization tests in deaerated reference solution, 1 M  $Na_2SO_4$  and 1 M  $Na_2S_2O_3$  solution, respectively.

### 2. Experimental Methods

#### 2.1. Preparation of magnetite deposited specimens

Mill-annealed Alloy 600 was used as a test material. The specimens were prepared with the same surface roughness using 1000 grit SiC papers. A magnetite working electrode was prepared by electrodeposition of magnetite layer on the entire surface of an Alloy 600 working electrode. The electrodeposition solution consisted of 2 M NaOH, 0.1 M triethanolamine and 0.043 M  $Fe_2(SO_4)_3$ . The electrodeposition of magnetite layer was conducted at an applied potential of  $-1.05 V_{SCE}$  for 30 min at  $80^\circ C$ .

#### 2.2. Polarization tests

To evaluate the effect of sulfate and thiosulfate solution, three types of test solutions were prepared. A reference solution of pH 9.0 at  $25^\circ C$  was prepared using NaOH as a pH adjuster, and 1 M  $Na_2SO_4$ , 1 M  $Na_2S_2O_3$  were added to the reference solution, respectively. Polarization tests were conducted using a potentiostat and a three-electrode cell. A saturated calomel electrode and platinum wire were used as a reference and counter electrode, respectively. The test solution was purged continuously using high purity nitrogen gas (99.98%) at a rate of  $100 \text{ cm}^3/\text{min}$  until the test was over. Open-circuit potential (OCP) was stabilized for 1 hour and then cathodic or anodic tests were conducted at a scan rate of  $0.5 \text{ mV/s}$ .

### 3. Results and Discussion

Fig. 1 shows the SEM images of the magnetite specimen prepared by the electrodeposition method. As shown in Fig. 1(a), the electrodeposited magnetite surface had highly faceted and dense morphology. As shown in Fig. 1(b), the cross section of the magnetite constituted a dense layer where no defects such as cracks or holes were observed. This means that the magnetite layer is tightly attached to the Alloy 600 substrate. Thus, it is considered to be useful for evaluating the electrochemical behavior of magnetite. The average thickness of the magnetite layer was approximately  $10 \mu\text{m}$ .

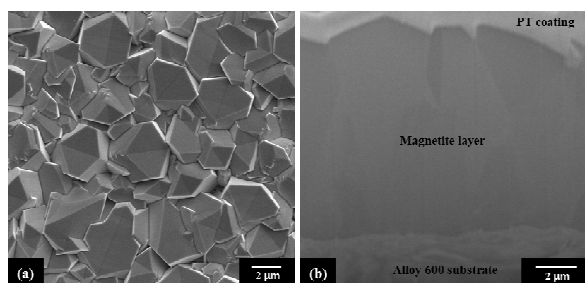


Fig. 1. SEM images of magnetite layer electrodeposited on Alloy 600: (a) top view and (b) cross section.

Fig. 2 shows the polarization curves of Alloy 600 and magnetite in the reference solution without sulfur species at 80°C. The  $i_{\text{corr}}$  of Alloy 600 and magnetite at the individual OCPs were  $0.42 \mu\text{A}/\text{cm}^2$  and  $1.41 \mu\text{A}/\text{cm}^2$ , respectively. The  $E_{\text{corr}}$  of Alloy 600 was about 100 mV lower than that of magnetite. This indicates that Alloy 600 behaves as an anode when Alloy 600 and magnetite are electrically connected. Therefore, if these two materials are electrically connected with the same area ratio, the anodic dissolution rate of Alloy 600 is expected to increase from  $0.42 \mu\text{A}/\text{cm}^2$  to  $1.07 \mu\text{A}/\text{cm}^2$ . However, since the area ratio (AR) of magnetite to Alloy 600 is much larger than 1 in actual environments, it is considered that the anodic dissolution rate of Alloy 600 will be further increased. The polarization curve of magnetite with an area of  $30 \text{ cm}^2$  was also presented in Fig. 2. Therefore, the anodic dissolution rate of Alloy 600 is expected to increase from  $0.42 \mu\text{A}/\text{cm}^2$  to  $1.65 \mu\text{A}/\text{cm}^2$  at an AR of 30.

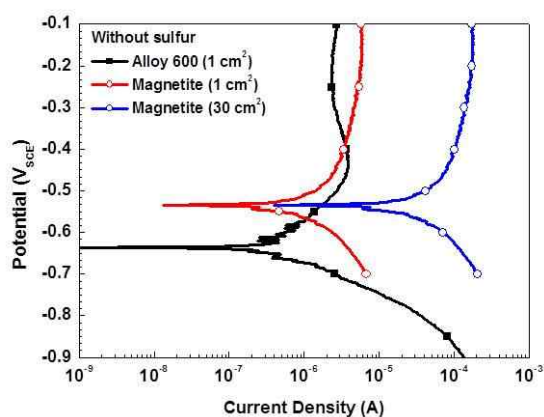


Fig. 2. Polarization curves of Alloy 600 and magnetite in reference solution of pH 9.0 at 80°C.

Fig. 3 shows the polarization curves of Alloy 600 and magnetite in the reference solution with 1 M  $\text{Na}_2\text{SO}_4$  at 80°C. The  $i_{\text{corr}}$  of Alloy 600 and magnetite at the individual OCPs were  $0.41 \mu\text{A}/\text{cm}^2$  and  $0.73 \mu\text{A}/\text{cm}^2$ , respectively. The  $E_{\text{corr}}$  of Alloy 600 was about 150 mV lower than that of magnetite. The difference of  $E_{\text{corr}}$  between the two materials in reference solution was

about 100 mV, but it increased to 150 mV in 1 M  $\text{Na}_2\text{SO}_4$  solution. If these two materials are electrically connected with the same area ratio, the anodic dissolution rate of Alloy 600 is expected to increase from  $0.41 \mu\text{A}/\text{cm}^2$  to  $1.83 \mu\text{A}/\text{cm}^2$ . However, as mentioned previously, the area ratio between Alloy 600 and magnetite in the actual crevice environments is not the same. Because porous magnetite is deposited on the surface of Alloy 600 tubing, a galvanic couple with an unfavorably large area ratio of a large cathode (magnetite) to a small anode (Alloy 600) is formed. The polarization curves of magnetite with an area of  $30 \text{ cm}^2$  was also superimposed in Fig. 3. In this case, the anodic dissolution rate of Alloy 600 is expected to increase from  $0.41 \mu\text{A}/\text{cm}^2$  to  $2.43 \mu\text{A}/\text{cm}^2$ .

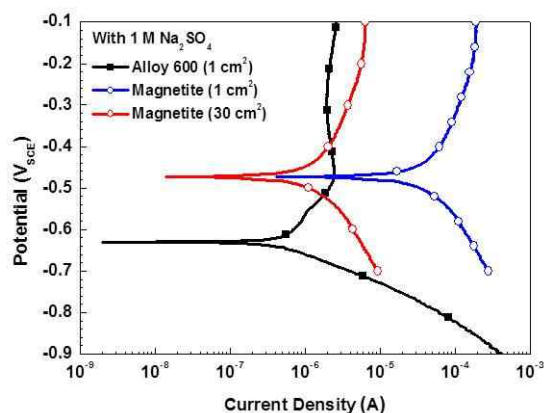


Fig. 3. Polarization curves of Alloy 600 and magnetite in reference solution of pH 9.0 with 1 M  $\text{Na}_2\text{SO}_4$  at 80°C.

Fig. 4 shows the polarization curves of Alloy 600 and magnetite in the reference solution with 1 M  $\text{Na}_2\text{S}_2\text{O}_3$  at 80°C. The  $i_{\text{corr}}$  of Alloy 600 and magnetite at the individual OCPs were  $0.25 \mu\text{A}/\text{cm}^2$  and  $0.84 \mu\text{A}/\text{cm}^2$ , respectively. The  $E_{\text{corr}}$  of Alloy 600 was about 90 mV higher than that of magnetite. Unlike previous two results, polarization behavior in 1 M  $\text{Na}_2\text{S}_2\text{O}_3$  solution showed a different result. When the Alloy 600 and magnetite are galvanically coupled in reference solution and 1 M  $\text{Na}_2\text{SO}_4$  solution, Alloy 600 and magnetite will behave as an anode and a cathode, respectively. However, this electrochemical behavior is reversed in solution containing 1 M  $\text{Na}_2\text{S}_2\text{O}_3$ . Therefore, it is considered that the galvanic corrosion between Alloy 600 and magnetite is not affected although the Alloy 600 is electrochemically coupled to magnetite in the solution containing 1 M thiosulfate.

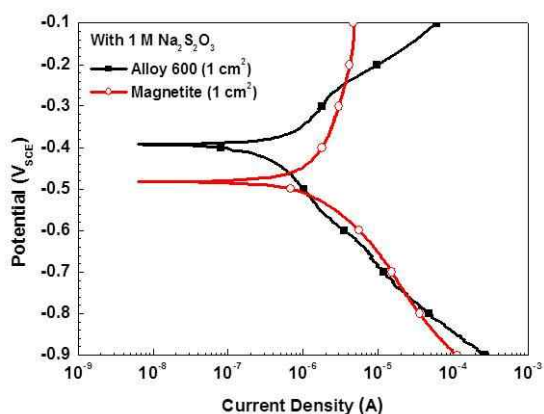


Fig. 4. Polarization curves of Alloy 600 and magnetite in reference solution of pH 9.0 with 1 M  $\text{Na}_2\text{S}_2\text{O}_3$  at  $80^\circ\text{C}$ .

Fig. 5 shows the change in the corrosion current of Alloy 600 calculated from the polarization curves of Figs. 2 and 3. When Alloy 600 was not galvanically connected with magnetite, there was almost no difference in the corrosion current density in reference solution and sulfate solution. However, when Alloy 600 and magnetite are galvanically connected, the corrosion current density of Alloy 600 will be increased. In addition, the corrosion current density of Alloy 600 was further increased in sulfate solution. This means that the galvanic effect with magnetite is more increased in sulfate solution. Furthermore, as the AR of magnetite to Alloy 600 increased, the corrosion current density in the sulfate solution was also higher than that in reference solution.

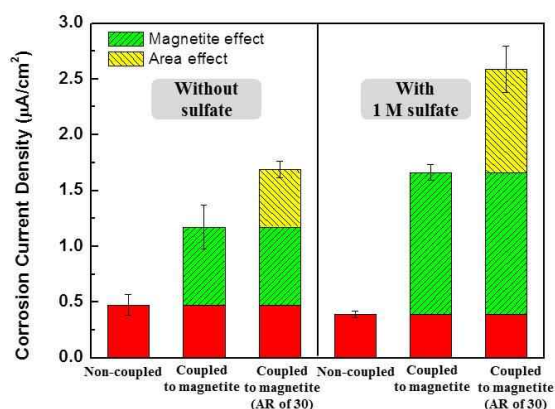


Fig. 5. Change in the anodic dissolution rate of Alloy 600 by the effect of magnetite and sulfate ion at  $80^\circ\text{C}$ .

#### 4. Conclusions

Polarization tests were conducted to investigate the electrochemical behavior of Alloy 600 and magnetite in reference solution, 1 M  $\text{Na}_2\text{SO}_4$  and 1 M  $\text{Na}_2\text{S}_2\text{O}_3$  solution. The tentative conclusions can be drawn as follows.

- (1) When Alloy 600 and magnetite were connected to form a galvanic coupling, the anodic dissolution rate of Alloy 600 was increased. Furthermore, the anodic dissolution rate of Alloy 600 in sulfate solution was more increased.
- (2) The increased galvanic corrosion of Alloy 600 was not expected in the solution containing thiosulfate although Alloy 600 was electrochemically coupled to magnetite.
- (3) From these electrochemical results, the effects of not only impurities but also magnetite should be considered as an acceleration factor on the corrosion of steam generator tubes.

#### ACKNOWLEDGEMENTS

This work was supported by the National Research Foundation of Korea (NRF) grant funded by the Korea government (2017M2A8A4015159).

#### REFERENCES

- [1] M. Basset, Deposition of Magnetite Particles onto Alloy-800 Steam Generator Tubes, IAEA, International steam generator and heat exchanger conference, pp. 677-693, 1998.
- [2] R.L. Tapping, C.W. Turner, R.H. Thompson, Steam Generator Deposits – A Detailed Analysis and Some Inferences, Corrosion, Vol. 47, No. 6, pp. 489-495, 1991.
- [3] R.W. Staehle, J.A. Gorman, Quantitative Assessment of Submodes of Stress Corrosion Cracking on the Secondary Side of Steam Generator Tubing in Pressurized Water Reactors, Corrosion, Vol. 59, No. 11, pp. 931-994, 2003.
- [4] I.J. Yang, Effect Sulphate and Chloride ions on the Crevice Chemistry and Stress Corrosion Cracking of Alloy 600 in High Temperature Aqueous Solutions, Corrosion Science, Vol. 33, No. 1, pp. 25-37, 1992.
- [5] EPRI, Laboratory Program to Examine Effects of Layup Conditions on Pitting of Alloy 600, Research Project S124-1 Final Report NP-3012, 1983.
- [6] EPRI, Pressurized Water Reactor Secondary Water Chemistry Guidelines – Revision 7, pp. 197, 2009.
- [7] G.D. Song, S.H. Jeon, J.G. Kim, D.H. Hur, Effect of polyacrylic acid on the corrosion behavior of carbon steel and magnetite in alkaline aqueous solutions, Corrosion 72 (2016) 1010-1120.
- [8] S.H. Jeon, G.D. Song, D.H. Hur, Corrosion behavior of Alloy 600 coupled with electrodeposited magnetite in simulated secondary water of PWRs, Mater. Trans. 56 (2015) 2078-2083.
- [9] S.H. Jeon, G.D. Song, D.H. Hur, Electrodeposition of magnetite on carbon steel in Fe(III)-triethanolamine solution and its corrosion behavior, Mater. Trans. 56 (2015) 1107-1111.
- [10] S.H. Jeon, G.D. Song, D.H. Hur, Galvanic corrosion between Alloy 690 and magnetite in alkaline aqueous solutions, Metals 5 (2015) 2372-2382.
- [11] G.D. Song, S.H. Jeon, J.G. Kim, D.H. Hur, Corrosion Science, Galvanic effect of magnetite on the corrosion behavior of carbon steel in deaerated alkaline solutions under flowing conditions, Corrosion Science 131 (2018) 71-80.

[12] G.D. Song, S.H. Jeon, J.G. Kim, D.H. Hur, Synergistic Effect of Chloride Ions and Magnetite on the Corrosion of Alloy 690 in Alkaline Solution, *Corrosion*, Vol. 73, No. 3, pp. 216-220, 2017.